Food and Chemical Toxicology 127 (2019) 19–30

Contents lists available at ScienceDirect

Food and Chemical Toxicology

journal homepage: www.elsevier.com/locate/foodchemtox

Hesperidin structurally modified by gamma irradiation induces apoptosis in murine melanoma B16BL6 cells and inhibits both subcutaneous tumor growth and metastasis in C57BL/6 mice

Eui-Baek Byun[a,*], Hye-Min Kim[a,b], Ha-Yeon Song[a,c], Woo Sik Kim[a]

[a] Advanced Radiation Technology Institute, Korea Atomic Energy Research Institute, Jeongeup, 56212, Republic of Korea
[b] Department of Food and Biotechnology, Korea University, Sejong, 30019, Republic of Korea
[c] Department of Biotechnology, College of Life Science and Biotechnology, Korea University, Seoul, 02841, Republic of Korea

ARTICLE INFO

Keywords:
Gamma irradiation
Hesperidin
Apoptosis
Tumor growth
Metastasis

ABSTRACT

Hesperidin is a flavonoid which occurs in citrus fruits. Hesperidin was gamma-irradiated at doses of 0, 30, 70, and 150 kGy. Gamma irradiation induced a decreased hesperidin peak, and a new radiolytic peak that gradually increased up to 150 kGy. The new radiolytic peak was fractionated, and the fractionated hesperidin derivative was used for subsequent experiments. Hesperidin gamma-irradiated at 150 kGy was toxic toward B16BL6 cells, but not toward bone marrow-derived macrophages. This cytotoxicity was exerted via induction of apoptosis, as reflected by the high population of double-positive cells, increased sub-G1 phase cells, depolarization of matrix metalloproteinase, production of reactive oxygen species, weakness of cell adhesion, changes in cell morphology, and inhibition of B16BL6 cell migration. Furthermore, 150 kGy gamma-irradiated hesperidin decreased the expression of Bcl-2 and pro-caspases-3 and -9, increased the expression of Bax and cytosolic cytochrome *c*, and increased the cleavage of poly ADP ribose polymerase. *In vitro* mechanistic study revealed that 150 kGy gamma-irradiated hesperidin achieved significantly greater inhibition of lung metastasis and growth of melanoma B16BL6 cells in C57BL/6 mice than non-irradiated intact hesperidin did. These results suggest that the structural modification of hesperidin induced by gamma irradiation could facilitate the development of anti-cancer drugs.

1. Introduction

Interest in natural compounds, such as polyphenols derived from plants, has been growing because of the many reports indicating the biological potential of these compounds (Bi et al., 2005; Delmas et al., 2005; Lastra and Villegas, 2005). Hesperidin is a bioflavonoid found in many citrus fruits including sweet orange, mandarin, lemon and lime. A wide range of pharmacological effects of hesperidin on atherosclerosis, inflammatory diseases, aging, cancer, virus disease, allergy, and nerve injury have been described (Chen et al., 2010; Filho et al., 2013; Garg et al., 2001; So et al., 1996).

Epidemiological and clinical investigations have revealed that among human pathologies, cancer is a major cause of death worldwide (Beckett, 1993; Cheung et al., 2008; Gill et al., 2008). In this context, cell death, particularly apoptosis, which occurs during the course of various physiological and pathological conditions, offers a promising therapeutic approach (Ouyang et al., 2012; Wong, 2011). Hesperidin exhibits strong anti-cancer activity by inducing apoptotic effects on breast cancer cells, prostate cancer cells, human colon cancer cells, and lymphoma cancer cells (Ghorbani et al., 2012; Lee et al., 2010; Natarajan et al., 2011; Park et al., 2008). Furthermore, hesperidin may induce apoptosis via mitochondrial and death receptor pathways, involving B-cell lymphoma-2 (Bcl-2), Bcl-2-associated X protein (Bax), caspase-3, and caspase-9 activation, in SNU-C4 human colon cancer cells and human hepatocellular carcinoma cells (Banjerdpongchai et al., 2016; Park et al., 2008).

Apoptosis is a physiological means to eliminate cancer cells without harming normal cells or tissues. Apoptosis has been explored as the basis of the anti-cancer activity of various potentially therapeutic compounds (Ouyang et al., 2012; Wong, 2011). Many studies have

Abbreviations: MTT, 3-(4,5-dimethylthiazol-2-yl)-2,5-diphenyl tetrazolium bromide; DCFH-DA, 2′,7′-Dichlorodihydrofluorescein diacetate; JC-1, 5,5′,6,6′-tetrachloro-1,1′,3,3′-tetraethyl-benzimidazolylcarbocyanine chloride; Bcl-2, B-cell lymphoma-2; Bax, Bcl-2-associated X protein; PARP, Poly ADP ribose polymerases; MMP, mitochondrial membrane potential; H&E, hematoxylin and eosin

* Corresponding author. Advanced Radiation Technology Institute, Korea Atomic Energy Research Institute, Jeongeup, 580-185, Republic of Korea. Tel.: +82 063 570 3245; fax: +82 063 570 3371.
E-mail address: ebbyun80@gmail.com (E.-B. Byun).

https://doi.org/10.1016/j.fct.2019.02.042
Received 15 October 2018; Received in revised form 25 February 2019; Accepted 27 February 2019
Available online 04 March 2019
0278-6915/

investigated the biological activity of natural compounds as anti-cancer agents. Ingestion of natural products at high concentrations has resulted in side effects, such as cytotoxicity, which damages normal cells and tissues (Mennen et al., 2005). As a solution, radiation technology was used to structurally modify natural compounds to reduce cytotoxicity and improve physiological activity. We previously demonstrated the use of gamma irradiation to improve physiological activity by structurally modifying various natural molecules that included fucoidan, silk protein, mistletoe, and β-glucan (Byun et al., 2010; Choi and Kim, 2013; Sung et al., 2009, 2013). In particular, gamma-irradiated polyphenols, such as genistein, quercetin, apigenin, resveratrol, and aloe-emodin, displayed reduced toxicity to normal cells or tissues, and improved physiological activities including anti-inflammatory and anti-cancer actions (Byun et al., 2015, 2017, 2018; Park et al., 2015; Sung et al., 2014).

In the past, the trend in radiation technology research was directed toward the application of radiation to sterilize medical supplies and food, as well as for the diagnosis and treatment of a wide variety of human pathological processes (Lee et al., 2005; Micke et al., 2002; Seegenschmiedt et al., 2000). However, the present focus has shifted to various biological and pharmaceutical applications. We provide novel, first-hand insights into the potential therapeutic value of radiation-mediated structural modification of natural biomaterials to reduce cytotoxicity and improve physiological activity of the biomaterials. The objective of this study was to evaluate the anti-cancer potential of gamma-irradiated hesperidin using *in vitro* and *in vivo* models to identify the effects on structural modification and improved activity.

2. Materials and methods

2.1. Materials

Hesperidin, MTT (3-(4, 5-dimethylthiazol-2-yl)-2,5-diphenyl tetrazolium bromide), Hoechst 33258 solution (bis-benzimide) and DCFH-DA (2′,7′-dichlorodihydrofluorescein diacetate) were obtained from Sigma-Aldrich (St. Louis, MO, USA). The fluorescein isothiocyanate (FITC)-annexin V/propidium iodide (PI) apoptosis detection kit was purchased from BD PharMingen (San Jose, CA, USA). The 5,5′,6,6′-tetrachloro-1,1′,3,3′-tetraethyl-benzimidazolylcarbocyanine chloride (JC-1) mitochondrial membrane potential kit was purchased from Cell Technology (Minneapolis, MN, USA). Antibodies for Bcl-2, Bax, caspase-3, caspase-9, poly ADP ribose polymerase (PARP), cytochrome c, and β-actin were obtained from Cell Signaling Technology (Danvers, MA, USA).

2.2. Gamma irradiation

Hesperidin was dissolved in dimethylsulfoxide (DMSO, Sigma-Aldrich) to obtain a concentration of 1 mg/mL (w/v). The hesperidin solution was irradiated at 30, 70, and 150 kGy in a cobalt-60 irradiator (point source AECL, IR-79; MDS Nordion International Co., Ltd, Ottawa, Ontario, Canada) equipped with a 11.1 PBq source strength at 10 ± 0.5 °C and operated at a dose rate of 10 kGy/h in the Advanced Radiation Technology Institute, a branch of the Korea Atomic Energy Research Institute (Jeoung-Eup, Korea). Dosimetry was performed using 5 mm-diameter alanine dosimeters (Bruker Instruments, Rheinstetten, Germany). The dosimeters were calibrated against an international standard set by the International Atomic Energy Agency (Vienna, Austria).

2.3. Structural analysis of gamma-irradiated hesperidin

A high-performance liquid chromatography (HPLC) system (1260 series; Agilent Technologies, Inc., Santa Clara, CA, USA) with a diode array detector was used to detect the degradation patterns of irradiated hesperidin. All samples were filtered prior to analysis using HPLC. The injection volume of gamma-irradiated and intact hesperidin (3 mg/mL) was 20 μL. The reverse phase Agilent Eclipse XDB–C18 column (5 μM pore size and length I.D., 4.6 mm × 250 mm) was operated using a mobile phase consisting of 0.1% acetic acid in water (A) and 0.1% acetic acid in acetonitrile (B) with a flow rate of 1 mL/min. An ultraviolet detector was used at a wavelength of 214 nm. The analyses were conducted in the gradient mode. The gradient program consisted of 0 min (10% B), 15 min (30% B), and 30 min (80% B). Purification was performed by preparative-HPLC (1260 Infinity System, Agilent) with the same gradient mode.

2.4. Cell culture

The B16BL6 murine melanoma cancer cell line was purchased from the Korean Cell Line Bank (KCLB, Seoul, Korea). The cells were cultured in Dulbecco's modified Eagle's medium (DMEM; GIBCO, Carlsbad, CA, USA) containing 10% fetal bovine serum (FBS, GIBCO), 100 U/mL penicillin, and 100 U/mL streptomycin in a humidified incubator at 37 °C in an atmosphere of 5% CO_2.

2.5. Animals

Six-week-old male C57BL6 mice (body weight 17–19 g) were purchased from ORIENT Bio Inc. (Seongnam, Korea). All animals received care in accordance with methods approved under institutional guidelines, and the study conformed to the principles of the 'Animal Care Act,' promulgated by the Ministry of Agriculture and Forestry, Republic of Korea. Experimental protocols were also approved by the Animal Ethics Committee of the Korea Atomic Energy Research Institute (KAERI-IACUC-2015-032).

2.6. Cytotoxicity

Cytotoxicity was measured using the MTT assay. B16BL6 cells were seeded in 96-well tissue culture plates and were treated with non-irradiated or 150 kGy gamma-irradiated hesperidin at 37 °C in the aforementioned 5% CO_2 incubator. After 24 h, MTT reagent was added to each well and the plates were incubated for a further 2–4 h. The supernatant was removed and DMSO was added to each well to dissolve the formazan crystals. Each well was evaluated using an ELISA plate reader (Zenyth 3100; Anthos Labtec Instruments GmbH, Salzburg, Austria) at a wavelength of 570 nm.

2.7. Apoptosis

Flow cytometry was performed to identify and quantify apoptotic cells using Annexin V/PI staining. B16BL6 cells were seeded in 6-well plates after treatment with gamma-irradiated and non-irradiated (intact) hesperidin at concentrations of 25 and 50 μg/mL for 24 h. Adherent cells were released by trypsin treatment. Both the adherent and floating cell populations were collected and washed twice with phosphate-buffered saline (PBS, pH 7.4; Invitrogen Inc., Carlsbad, CA, USA) and then subjected to Annexin V and PI staining using an Annexin V-FITC/PI apoptosis detection kit (BD PharMingen, San Jose, CA, USA) according to the manufacturer's instructions. After staining, apoptotic cells were quantified using a Becton-Dickinson FACS-Calibur flow cytometer.

2.8. Cell cycle analysis

Following treatment, cells were collected by trypsinization and centrifugation, washed with PBS, and fixed with 70% ethanol. Cells were labeled with PI solution (0.05 mg/mL PI, 2 mg/mL RNase A, 0.01% Triton X-100 in PBS) and incubated for 30 min at room temperature in darkness. Cell cycle (DNA content) was analyzed using a Becton-Dickinson FACS-Calibur flow cytometer.

2.9. Observation of morphological change

The toxic effect of samples during culture was visualized using a compact, inverted, optical microscope (LumaScope-620 Series; Etaluma, Carlsbad, CA, USA) equipped with a 40 × objective. Time-lapse images were captured and examined using time-lapsed capture images. The microscope was placed in the Heracell-240 incubator and connected to an external computer, which captured the images using LumaView600Cy 13.7.17.0 software (Etaluma). B16BL6 cells (10^4 per well) were seeded in the μ-Slide 2-well (Ibidi GmbH, Martinsried, Germany) and then treated with 0 and 150 kGy gamma-irradiated hesperidin. Formation of the cell monolayer was then monitored.

2.10. Hoechst 33258 staining

To observe the morphologic characteristics associated with apoptosis, B16BL6 cells were seeded in a 4-well culture slide chamber and treated with sample for 24 h. The cells were washed twice with PBS and stained with bis-benzimide (0.5 μg/mL) for 20 min at 37 °C. The fluorescence intensity in the cells was determined using confocal microscopy using a model LSM 800 microscope (Carl Zeiss, Oberkochen, Germany).

2.11. Mitochondrial membrane potential

Intracellular mitochondrial membrane potential (MMP) was assessed using the JC-1 stain according to the manufacturer's instructions. Briefly, following treatment, the cells were loaded with JC-1 staining solution for 15 min at 37 °C in the dark and washed once with assay buffer. Fluorescence intensity was measured using fluorescence microscopy at an excitation wavelength of 514 nm and emission wavelength of 529 nm for green fluorescence, and 585 nm and 590 nm excitation and emission wavelengths, respectively, for emission of red fluorescence.

2.12. Cell migration

Cells were seeded into each well of a 24-well plate and allowed to adhere overnight in an incubator at 37 °C. The medium was removed from each well, and the well surface was scraped gently with a sterilized wooden applicator stick (1 mm outer diameter; Baxter, McGaw Park, IL, USA) with the end of the stick in direct contact with the plate surface. This created a wound area for cell migration. Wells were gently washed with PBS. Supplemented medium and treated sample were added. The plates were re-incubated for 24 h. Cell migration was followed by microscopy.

2.13. Measurement of reactive oxygen species (ROS)

Production of intracellular ROS was detected via flow cytometry using DCFH-DA. B16BL6 cells were plated at a density of 1×10^5 cells/well for 24 h, and incubated with 100 μg/mL of hesperidin for 1, 3, 6, and 12 h. The wells were then stained with DCFH-DA (10 μM) for 20 min at 37 °C, and the fluorescence intensity in the cells was determined using flow cytometry and fluorescence microscopy.

2.14. Western blotting

B16BL6 cells were lysed in a buffer containing 50 mM Tris–HCl (pH 7.5), 150 mM NaCl, 1% Triton-X100, 1 mM EDTA, 50 mM NaF, 30 mM Na_4PO_7, 1 mM phenylmethylsulfonyl fluoride, 2 μg/mL aprotinin, and 1 mM pervanadate. The samples were separated via 10% SDS-PAGE and transferred onto polyvinylidene difluoride membranes. The membranes were blocked with 5% skim milk and incubated with each of the primary antibodies (1:1000) for 2 h, followed by incubation with horseradish peroxidase-conjugated secondary antibodies (1:2000) for 1 h at room temperature. Proteins were visualized using enhanced chemiluminescence (GE Healthcare, Little Chalfont, UK).

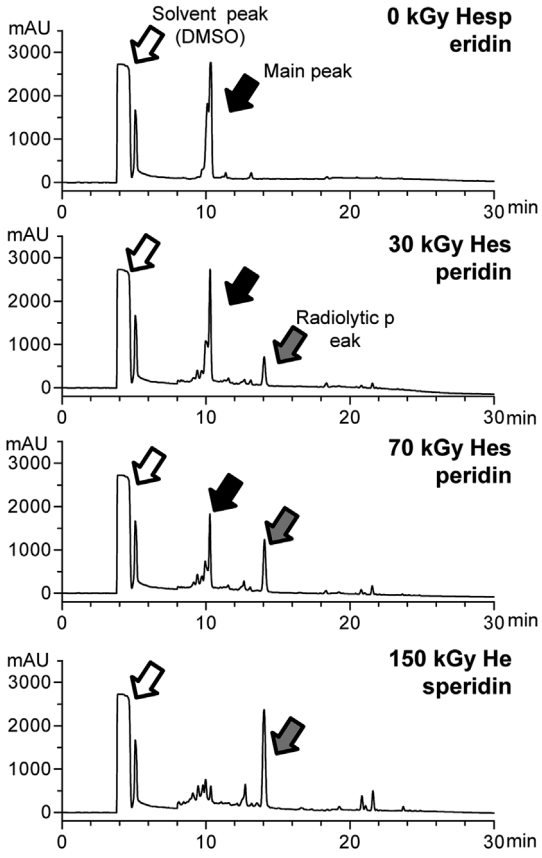

Fig. 1. Effects of gamma irradiation on hesperidin structure. Hesperidin was dissolved in dimethylsulfoxide (DMSO) and irradiated at doses of 30, 70, and 150 kGy. Structural modification of hesperidin was detected by HPLC.

2.15. Lung metastasis

B16BL6 cells (5×10^5 cells per animal) were injected into the tail veins of C57BL6 mice (four groups, n = 5 per group). First, intact and gamma-irradiated hesperidin was orally administered (2.5 mg each day) for 7 days before injection of tumor cells (preventive protocol). Intact and gamma-irradiated hesperidin were orally administered (2.5 mg each day) for 7 days after tumor cell injection (therapeutic protocol). Animals in the control group were given an equivalent volume of PBS. Some control mice died of lung metastasis approximately 3 weeks following the injection of B16BL6 cells. All mice were euthanized and examined. The spleen index was calculated as follows: Spleen index = (spleen weight/body weight) × 100.

2.16. Primary tumor growth

B16BL6 cells (5×10^5 cells per site) were injected into the backs of C57BL6 mice (four groups, n = 5 per group). First, intact and gamma-irradiated hesperidin were orally administered (2.5 mg each day) for 7 days before tumor cell injection (preventive protocol). Intact and gamma-irradiated hesperidin were orally administered (2.5 mg each day) for 7 days after tumor cell injection (therapeutic protocol). The controls received an equivalent volume of PBS. The mice were euthanized 14 days following tumor inoculation. The tumor colonies were separated from the mice and the tumor masses were weighed.

2.17. Histopathological analysis

Lungs were fixed in 10% formalin for histopathological analysis.

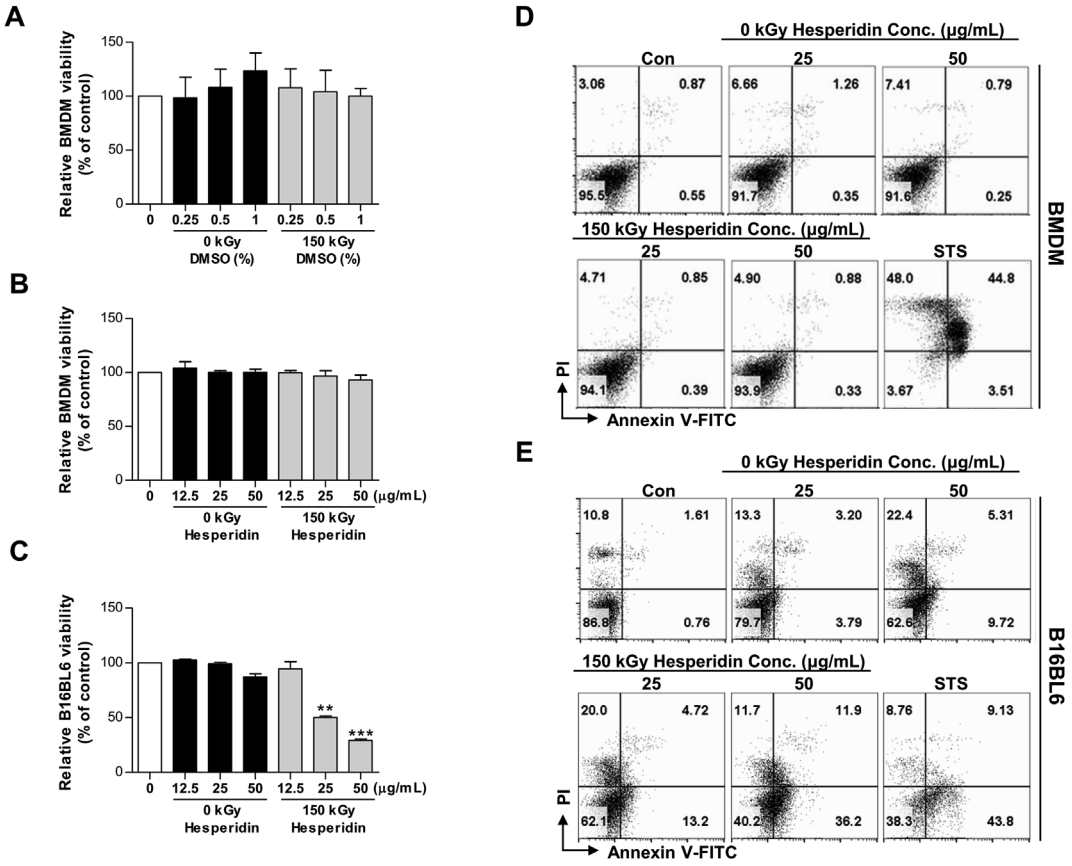

Fig. 2. Toxicity of gamma-irradiated hesperidin toward normal cells and tumor cells. Effect of DMSO (control) (A) or gamma-irradiated hesperidin on the viability of different cell types (BMDMs: B, B16BL6 melanoma cells: C) was measured using the MTT assay and annexin V/PI staining (D and E). Results are representative of three independent replicates. All bar graphs show mean ± SD. Significant differences were evaluated using unpaired Student's *t*-test within $^{**}p < 0.01$ and $^{***}p < 0.001$ compared with control group.

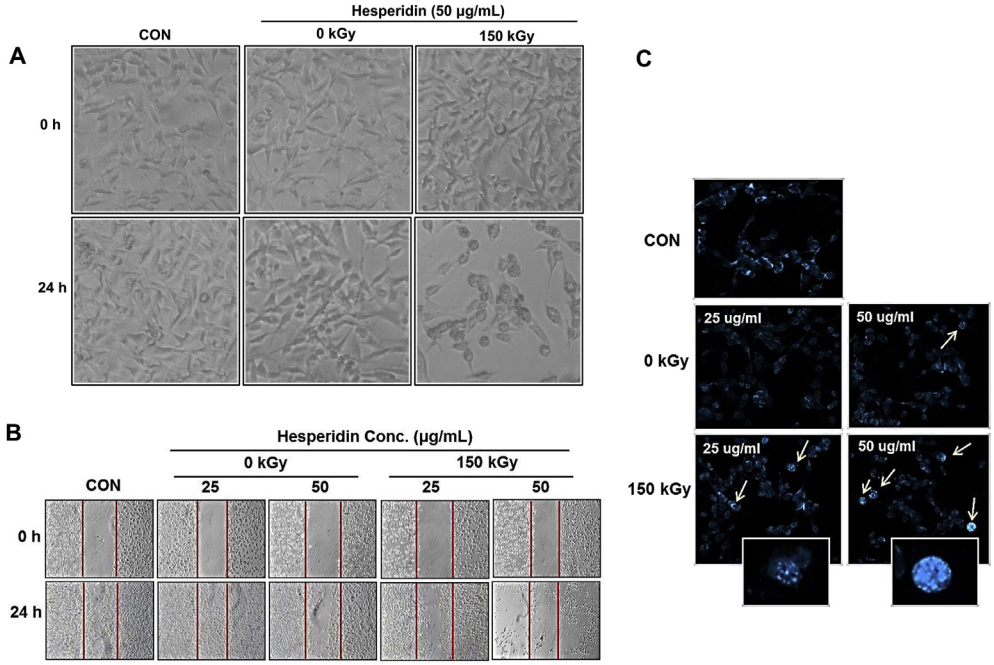

Fig. 3. Effects of gamma-irradiated hesperidin on morphology of B16BL6 melanoma cells. Morphological characteristics, i.e., size and shape (A), and migration ability (B) of gamma-irradiated hesperidin-treated cells were determined by microscopic observations. Apoptotic morphological changes (C) were examined by confocal microscopy using Hoechst 33258 staining.

The lung tissue was processed in ethanol followed by washing with xylene and embedding in paraffin. Five micrometer-thick sections were cut using a microtome (Leica Microsystems, Wetzlar, Germany). The sections were de-waxed and stained with hematoxylin and eosin (H&E). Slides containing the sections were observed using an Eclipse E 400 microscope (Nikon, Biberach, Germany) and photographed.

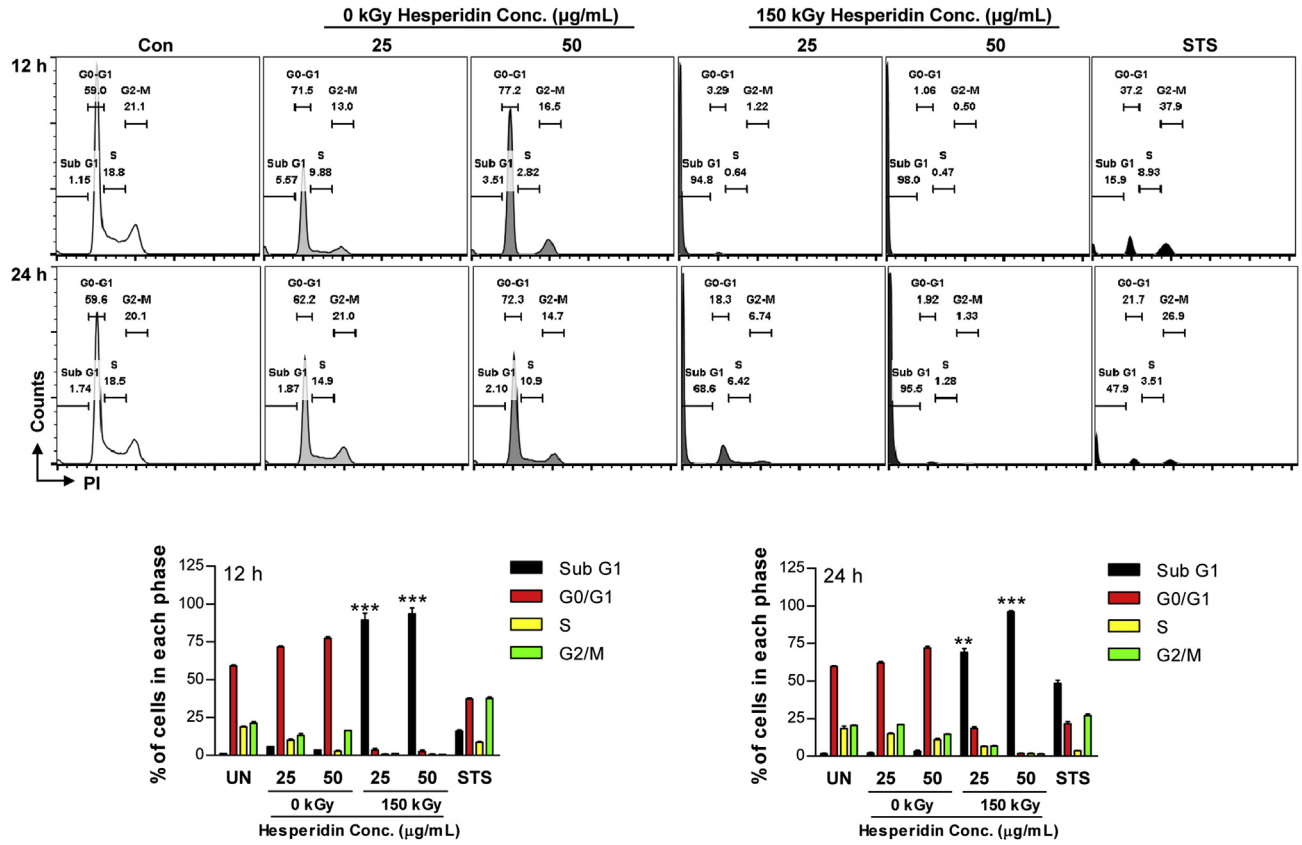

Fig. 4. Induction of cell cycle arrest by gamma-irradiated hesperidin in B16BL6 melanoma cells. Representative flow cytometry results of cell cycle distribution of subpopulation of control and gamma-irradiated (0 kGy or 150 kGy) hesperidin-treated B16BL6 melanoma cells. The bar graph denotes mean ± SD (n = 3 sample per group) of percentage of each phase in the cell cycle. Significance differences were evaluated using unpaired Student's *t*-test within $^{**}p < 0.01$ and $^{***}p < 0.001$ compared with control group.

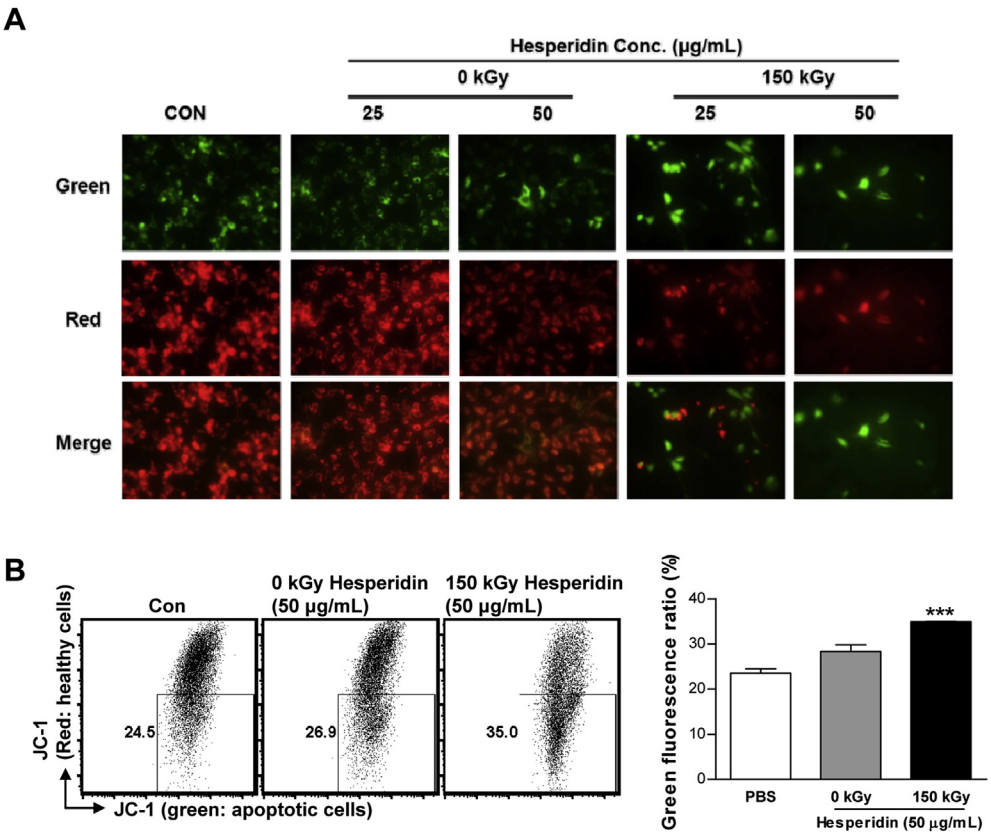

Fig. 5. Effects of gamma-irradiated hesperidin on mitochondrial membrane potential change in B16BL6 melanoma cells. (A and B) The cells were treated with 0 kGy intact hesperidin or 150 kGy hesperidin for 24 h, and then stained with JC-1 dye. The fluorescence shift was observed via fluorescence microscopy (A, × 20 magnification) and flow cytometry (B).

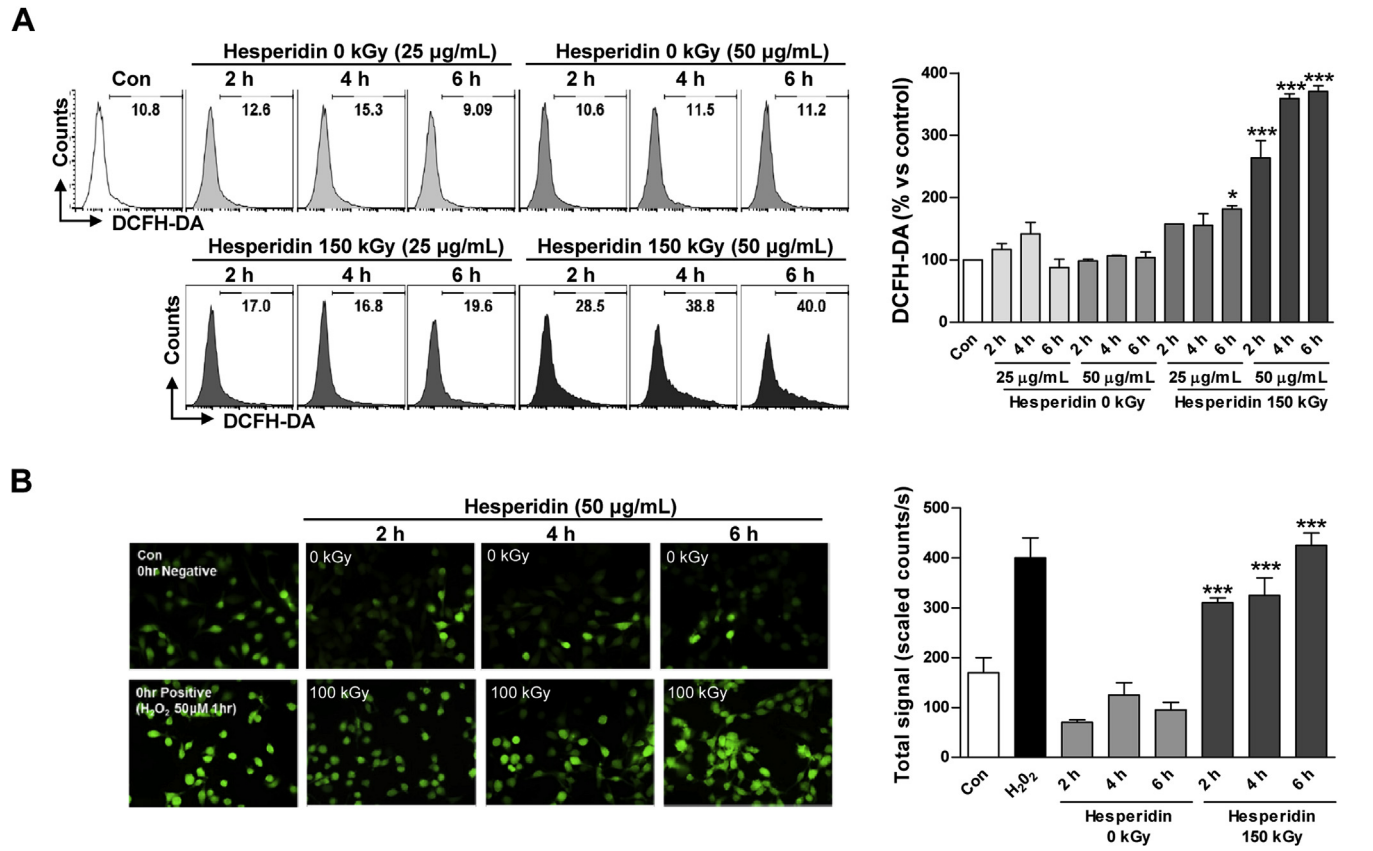

Fig. 6. Effects of gamma-irradiated hesperidin on the generation of reactive oxygen species (ROS) in B16BL6 melanoma cells. The cells were treated with 0 kGy intact hesperidin or 150 kGy hesperidin at the indicated times, and stained with DCFH-DA. Generation of ROS was observed via flow cytometry (A) and fluorescence microscopy (B). The bar graphs denote mean ± SD (n = 3 sample per group) of percentage of fluorescence. Significance differences were evaluated using unpaired Student's *t*-test within $^{*}p < 0.05$, $^{**}p < 0.01$ and $^{***}p < 0.001$ compared with the control group.

2.18. Statistical analyses

The means and standard deviations were calculated using SPSS software 18 (SPSS Inc., Chicago, IL, USA). Differences between means were examined using one way analysis of variance (ANOVA) and Student's two tailed *t*-test. The results are expressed as mean ± SD. Statistical significance was set at $^{*}p < 0.05$, $^{**}p < 0.01$, and $^{***}p < 0.001$.

3. Results

3.1. Analysis of structural change of hesperidin induced by gamma irradiation

The structural changes of hesperidin induced by gamma irradiation were analyzed by HPLC. Chromatograms of gamma-irradiated (30, 70, and 150 kGy) and intact (0 kGy) hesperidin are shown in Fig. 1. The main peak of hesperidin decreased gradually as the irradiation dose increased up to 150 kGy. Interestingly, radiation exposure was accompanied by the appearance of several new peaks. This result indicated that gamma irradiation might generate substantial structural modifications in hesperidin, in addition to producing new dose-dependent radiolytic peaks. The new radiolytic peak derived from 150 kGy gamma-irradiated hesperidin was fractionated using preparation-HPLC, and the fractionated hesperidin derivative (new radiolytic peak) was used for subsequent experiments. Next, we evaluated the anti-cancer activity in murine melanoma B16BL6 cancer cells to investigate whether the new radiolytic peak produced by gamma irradiation reflect changes in the physiological properties of hesperidin.

3.2. Gamma-irradiated hesperidin inhibits growth of murine melanoma B16BL6 cells

Viability of B16BL6 cells was measured to investigate whether DMSO used in dissolution of hesperidin affected cell proliferation. DMSO (0.25, 0.5, and 1%) was not cytotoxic (Fig. 2A). To investigate the increase in tumor growth inhibition in relation to dose, the survival of B16BL6 cells was tested at various doses (12.5, 25, and 50 μg/mL). The 150 kGy gamma-irradiated hesperidin induced greater dose-dependent inhibition of tumor cell growth than intact hesperidin (Fig. 2C and E). In the case of normal cells (bone marrow-derived macrophages; BMDMs) growth inhibition by 150 kGy gamma-irradiated hesperidin was similar to that induced by the intact hesperidin (Fig. 2B and D). These results strongly suggested that tumorigenic cells are much more sensitive to 150 kGy gamma-irradiated hesperidin treatment than non-tumorigenic cells.

3.3. Gamma-irradiated hesperidin induces apoptosis in murine melanoma B16BL6 cells

We investigated whether treatment with 150 kGy gamma-irradiated hesperidin inhibits B16BL6 cell growth. B16BL6 cells were treated with 150 kGy gamma-irradiated hesperidin at concentration of 50 μg/mL for 0 and 24 h. The effects of 150 kGy gamma-irradiated hesperidin on B16BL6 cell proliferation were determined by assessing morphological changes at the cellular level (Fig. 3A). The 150 kGy gamma-irradiated hesperidin treatment produced markedly greater morphological alterations in B16BL6 cells than the intact hesperidin treatment. As shown in Fig. 3A, while cells in the control group maintained their regular shape and size, B16BL6 cells treated with 50 μg/mL of 150 kGy

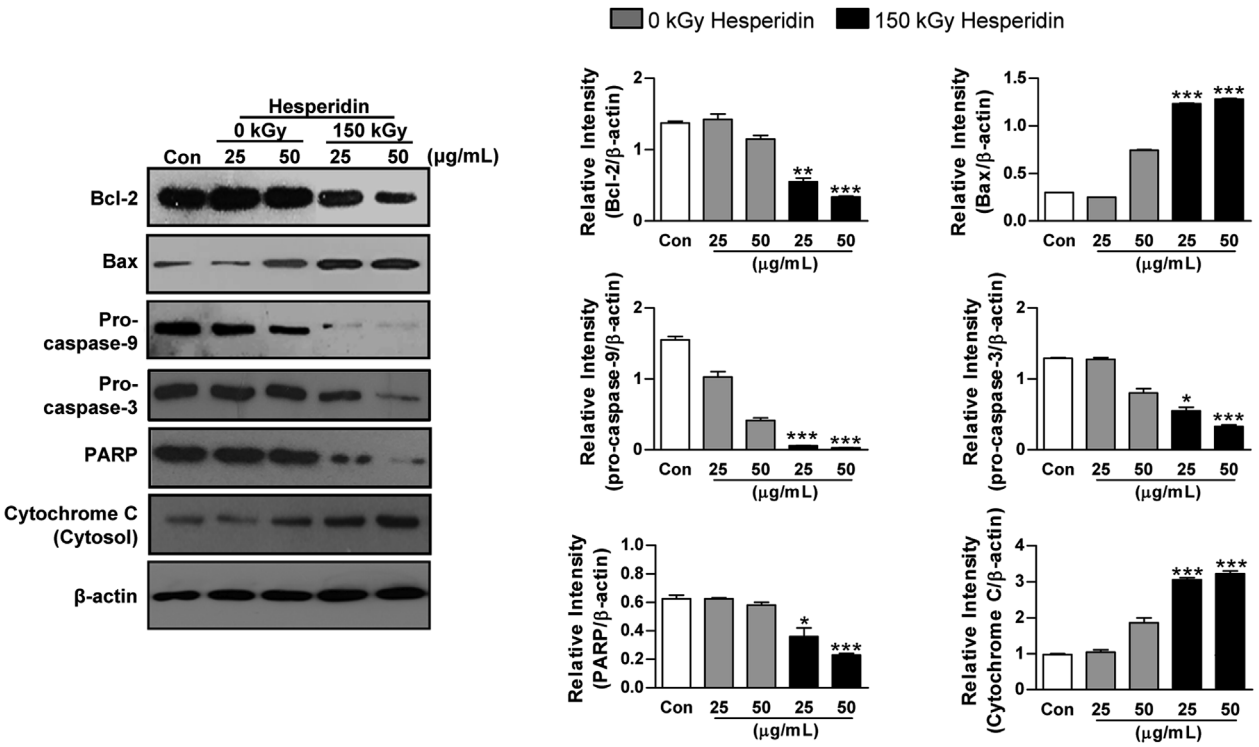

Fig. 7. Effects of gamma-irradiated hesperidin on mitochondria-dependent apoptotic pathways. The cells were treated with 0 kGy irradiated hesperidin or 150 kGy irradiated hesperidin for 24 h. The cell lysates were subjected to SDS-PAGE and western blot analyses using specific antibodies as indicated. The bar graphs show the relative band intensity of each protein. Significant differences were evaluated using unpaired Student's *t*-test within $^{*}p < 0.05$, $^{**}p < 0.01$ and $^{***}p < 0.001$ compared with the control group.

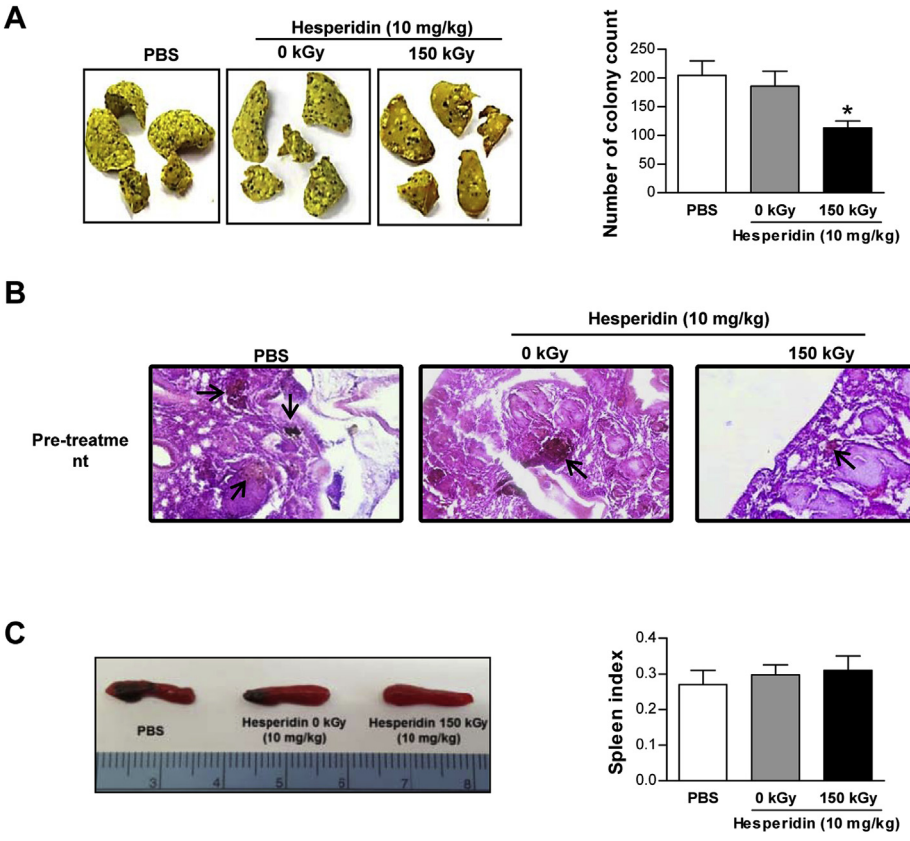

Fig. 8. Preventive effects of gamma-irradiated hesperidin on lung metastasis induced by intravenous injection of B16BL6 melanoma cells. Representative photographs of mouse lungs (A) and spleens (C) from each group of mice. (B) Representative histological images of lung tissue. The bar graph denotes the mean ± SD (n = 5 mice per group). Significant differences were evaluated using ANOVA followed by Tukey's multiple comparison test; $^{*}p < 0.05$ with PBS-treated group. Arrows indicate the B16 melanoma mass in the lung.

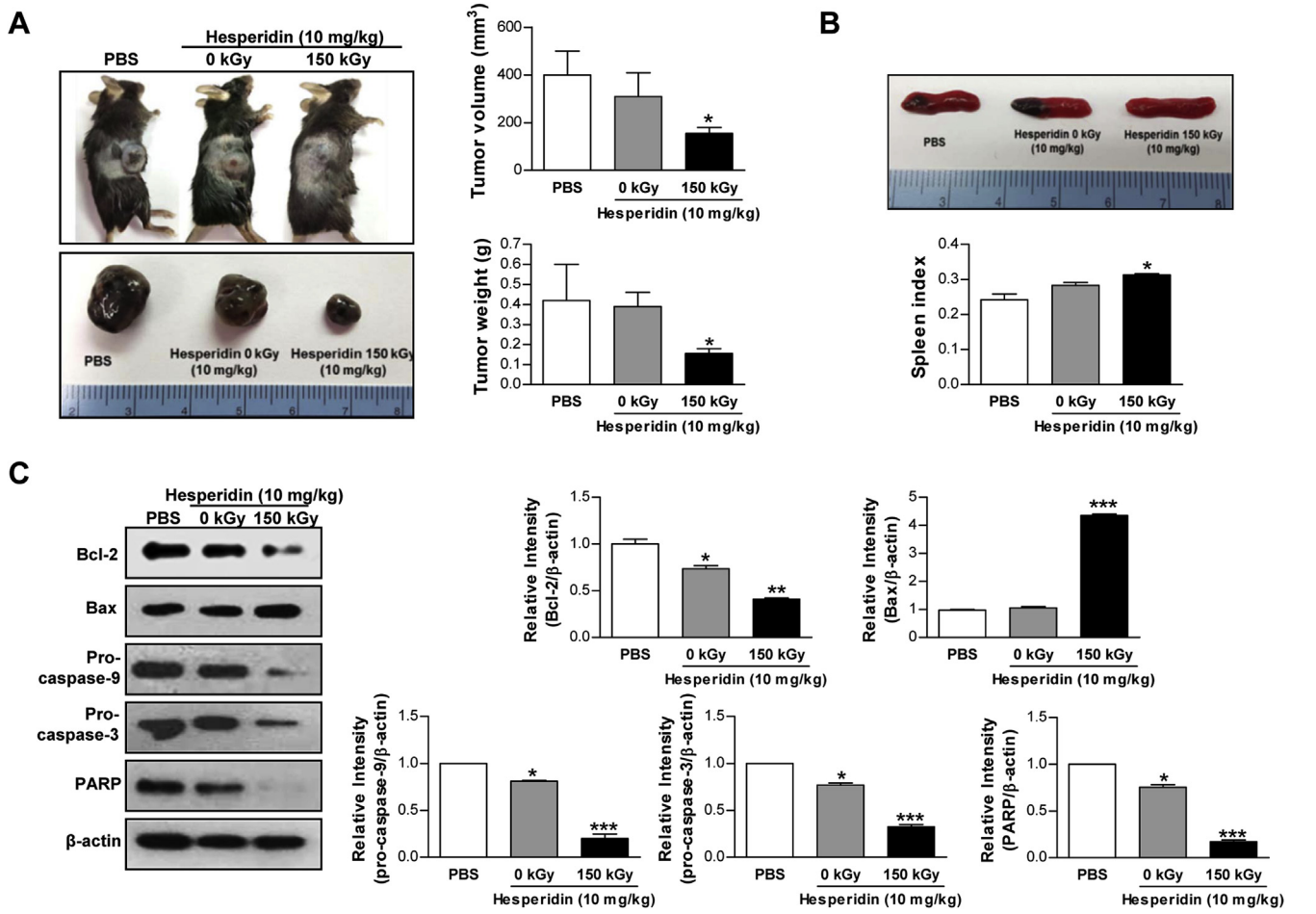

Fig. 9. Preventive effects of gamma-irradiated hesperidin on tumor growth induced by the subcutaneous injection of B16BL6 melanoma cells. Representative photographs of tumors (A) and spleens (B) from each group of mice. (C) Expression level of apoptosis-related protein in tumor tissue was determined by western blot analysis. The bar graph denotes mean ± SD (n = 5 mice per group). Significant differences were evaluated using ANOVA followed by Tukey's multiple comparison test; $^{*}p < 0.05$ with the PBS-treated group.

gamma-irradiated hesperidin were decreased in number and displayed irregular shapes and weakened cell adhesion, indicating altered morphology. Cell penetration through the filter was significantly decreased by the 150 kGy gamma-irradiated hesperidin treatment compared with that in the control (Fig. 3B). Furthermore, the 150 kGy gamma-irradiated hesperidin-treated B16BL6 cells showed significantly greater chromatin condensation and more apoptotic bodies than the control and intact hesperidin-treated cells (Fig. 3C). To determine whether 150 kGy gamma-irradiated hesperidin could induce apoptosis in B16BL6 cells, cell cycle analysis using flow cytometry was performed (Fig. 4). The proportion of the sub-G1 peak did not vary in the control and 150 kGy gamma-irradiated hesperidin treatment groups, whereas 12 and 24 h exposure of B16BL6 cells to 150 kGy gamma-irradiated hesperidin at 25 and 50 μg/mL increased the sub-G1 peak in time- and dose-dependent manners. These results strongly suggested that 150 kGy hesperidin could inhibit B16BL6 cell growth by inducing apoptosis.

3.4. Gamma-irradiated hesperidin improves MMP in murine melanoma B16BL6 cells

Apoptosis can be initiated through the intrinsic (mitochondrial) or extrinsic (receptor-mediated) pathways. The intrinsic pathway is triggered by intracellular signaling proteins (i.e., anti-apoptotic proteins, pro-apoptotic proteins, cytochrome *c*, poly ADP ribose polymerase (PARP), caspase-3, and -9, and others) and ROS production associated with mitochondrial membrane permeabilization (which is induced by irradiation or treatment with chemotherapeutic agents). The extrinsic pathway receives a signal from other cells to initiate apoptosis via membrane receptors (death receptors) in response to extracellular ligands (Gangopadhyay et al., 2014; Wu and Bratton, 2013; Wu et al., 2016). We focused on the intrinsic pathway that can be induced by treatment with chemotherapeutic agents. First, to examine changes in MMP, B16BL6 cells were stained with JC-1 and examined using inverted fluorescence microscopy (Fig. 5A) and flow cytometry (Fig. 5B). JC-1 aggregates in normal mitochondria and red fluorescence was indicative of a normal MMP. Exposure to 150 kGy gamma-irradiated hesperidin resulted in the dissipation of MMP, as shown by increased green fluorescence and decreased red fluorescence (Fig. 5A and B).

3.5. Gamma-irradiated hesperidin induces ROS generation in murine melanoma B16BL6 cells

ROS induce the intrinsic apoptotic signaling pathway in tumor cells (Wu and Bratton, 2013). We investigated whether 150 kGy gamma-irradiated hesperidin-induced apoptosis was correlated with ROS generation in B16BL6 cells. The irradiated hesperidin induced greater time- and dose-dependent increase in ROS generation by B16BL6 cells than did intact hesperidin (Fig. 6A and B). These results strongly indicated that 150 kGy gamma-irradiated hesperidin-induced cell death may be associated with ROS-mediated apoptosis signaling in murine melanoma B16BL6 cells.

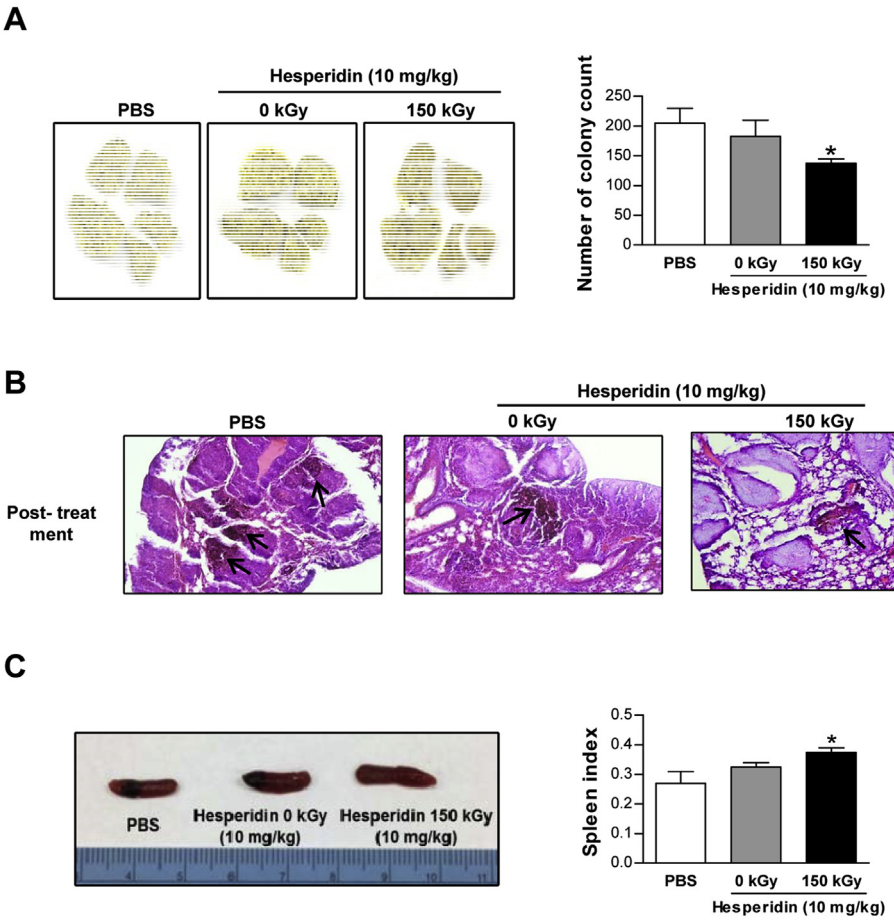

Fig. 10. Therapeutic effects of gamma-irradiated hesperidin on lung metastasis induced by intravenous injection of B16BL6 melanoma cells. Representative photographs of mouse lungs (A) and spleens (C) from each group of mice. (B) Representative histological images of lung tissue. The bar graph denotes mean ± SD (n = 5 mice per group). Significant differences were evaluated using ANOVA followed by Tukey's multiple comparison test; $^{*}p < 0.05$ with the PBS-treated group. Arrows indicate the B16 melanoma mass in the lung.

3.6. Mitochondrial apoptotic pathways are induced by gamma-irradiated hesperidin in murine melanoma B16BL6 cells

To determine whether 150 kGy gamma-irradiated hesperidin-induced apoptosis involves the intrinsic (mitochondrial) apoptotic signaling pathways, we evaluated the levels of pro-apoptotic protein (Bax) and anti-apoptotic protein (Bcl-2), cytosolic cytochrome *c* release, and the expressions of PARP, caspase-3, and caspase-9 (Fig. 7). B16BL6 cells treated with 150 kGy gamma-irradiated hesperidin showed higher Bax expression, lower Bcl-2 expression, and up-regulated cytosolic cytochrome *c* levels than those treated with intact hesperidin. Next, to examine whether pro-caspase-3 and -9, which lead to the respective activation of caspase-3 and -9, are involved in gamma-irradiated hesperidin-induced apoptosis, the expression levels of pro-caspase-3 and -9 were analyzed. B16BL6 cells exposed to 150 kGy gamma-irradiated hesperidin showed significantly higher expression of pro-caspase-3 and -9 than that in the intact hesperidin-treated group. Furthermore, greater increase in PARP cleavage was observed with 150 kGy gamma-irradiated hesperidin than with intact hesperidin. These findings suggest that the induction of gamma-irradiated hesperidin-induced apoptosis could be associated with the intrinsic apoptotic signaling pathways.

3.7. Gamma-irradiated hesperidin inhibits lung metastasis in vivo

To further define 150 kGy gamma-irradiated hesperidin-induced apoptosis in B16BL6 cells *in vitro*, we next studied the effects of 150 kGy gamma-irradiated hesperidin *in vivo* (lung metastasis) using a pre-treatment model (Fig. 8) and a post-treatment model (Fig. 10). As shown in Figs. 8A and 10A, oral treatment with 150 kGy gamma-irradiated hesperidin significantly reduced the number of lung nodules in C57BL6 mice injected intravenously with B16BL6 cells compared with those treated with intact hesperidin. Furthermore, histopathological analysis indicated that 150 kGy gamma-irradiated hesperidin treatment achieved more dramatic inhibition of lung metastasis of B16BL6 cells compared than intact hesperidin treatment (Figs. 8B and 10B). Additionally, the spleen index of mice the in post-treatment model was increased in the 150 kGy gamma-irradiated hesperidin treatment group (Fig. 10C), but not in the pre-treatment model (Fig. 8C). An increase or no significant difference of spleen index induced by pre- and post-treatment of gamma-irradiated hesperidin is expected to induce the immune cell recruitment and/or non-toxic effect for normal cells. These results indicated that 150 kGy gamma-irradiated hesperidin may inhibit lung metastasis of B16BL6 cells to a greater extent than intact hesperidin, without causing spleen damage.

3.8. Gamma-irradiated hesperidin inhibits tumor growth in vivo

We investigated the effect of gamma-irradiated hesperidin treatment (Fig. 9; pre-treatment, Fig. 11; post-treatment) on B16BL6-tumor growth models to confirm the gamma-irradiated hesperidin-induced cell death signals as well as tumor growth. Oral treatment with 150 kGy gamma-irradiated hesperidin significantly reduced the tumor growth in C57BL6 mice injected subcutaneously with B16BL6 cells compared to those treated with intact hesperidin (Figs. 9A and 11A). The evaluation of tumor growth was confirmed by tumor volume and weight. Additionally, the spleen index of mice in pre-treatment models increased in the 150 kGy gamma-irradiated hesperidin treatment group (Fig. 9B), but not in post-treatment setting (Fig. 11B). These results are consistent with the suggestion that gamma-irradiated hesperidin is more effective than intact hesperidin for inhibiting tumor growth. We finally investigated the levels of pro- and anti-apoptotic proteins in tumor lysates

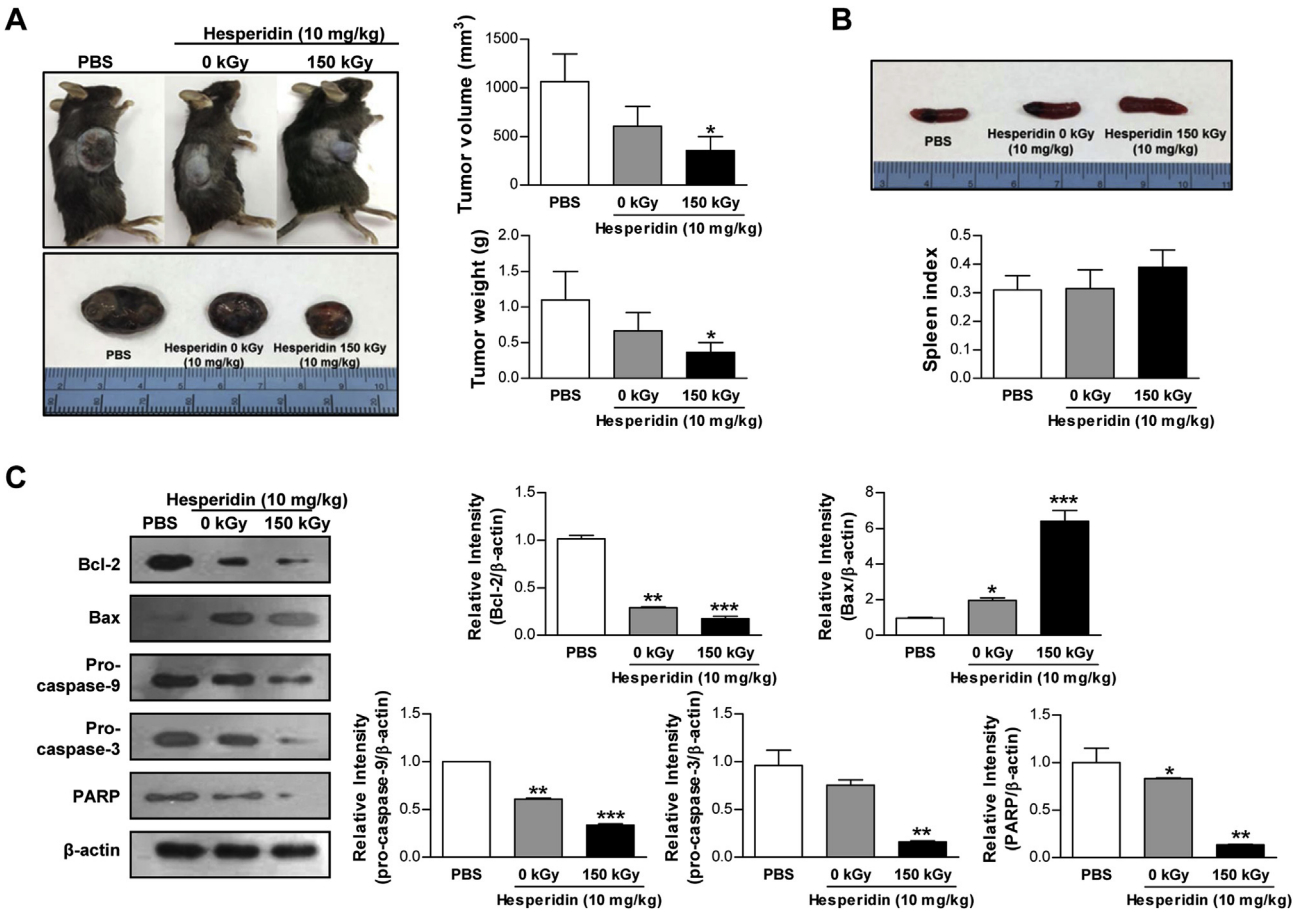

Fig. 11. Therapeutic effects of gamma-irradiated hesperidin on tumor growth induced by the subcutaneous injection of B16BL6 melanoma cells. Representative photographs of tumors (A) and spleens (B) from each group of mice. (C) Expression level of apoptosis-related protein in tumor tissue was determined by western blot analysis. The bar graph denotes mean ± SD ($n = 5$ mice per group). Significant differences were evaluated using ANOVA followed by Tukey's multiple comparison test; $^{*}p < 0.05$ with the PBS-treated group.

isolated from each mouse via western blot analysis. The 150 kGy gamma-irradiated hesperidin treatment groups significantly induced the expression of increased Bax and decreased Bcl-2, pro-caspase-3 and -9, and PARP (Figs. 9C and 11C). Therefore, the apoptotic action induced by gamma-irradiated hesperidin in B16BL6 cells *in vitro* was verified *in vivo* via the inhibition of lung metastasis and tumor growth under both pre- and post-treatment conditions.

4. Discussion and conclusion

Previous studies have investigated the biotransformation of biomaterials using enzymatic or heat-treatment methods to improve physiological properties through structural modification (Ilyina et al., 2000; Park et al., 1997). However, the disadvantages of these methods include high cost, low yield, and long processing times. Recent studies indicated that radiation technology may evenly modify the chemical structure of polyphenols, such as flavonol and isoflavone, through radical formation, leading ultimately to improved physiological properties (Byun et al., 2015; Jung et al., 2009). Hesperidin, the phenolic compound used in the present study, has also been reported to exhibit strong anti-cancer activity by inducing apoptosis in various cancers (Ghorbani et al., 2012; Lee et al., 2010; Natarajan et al., 2011; Park et al., 2008). However, hesperidin treatment at low concentrations (≤50 μg/mL) was not toxic to murine melanoma B16BL6 cells. Accordingly, in the present study, we attempted to modify the chemical structure of hesperidin using gamma irradiation to improve toxicity to murine melanoma B16BL6 cells. These efforts ultimately resulted in a new radiolytic peak at an irradiation dose of 150 kGy. This peak was fractionated using preparative-HPLC and the fractionated 150 kGy hesperidin was subsequently tested for anti-cancer activity *in vitro* and *in vivo*. As a first step, cytotoxicity of non-irradiated and 150 kGy gamma-irradiated hesperidin was examined in BMDMs (normal) and B16BL6 (melanoma) cells. The 150 kGy gamma-irradiated hesperidin treatment at 25–50 μg/mL showed significantly greater toxicity to B16BL6 cells than did intact hesperidin treatment, without inducing cytotoxic effects in BMDM cells. These findings may indicate that enhanced anti-cancer activity exhibited by gamma-irradiated hesperidin is closely associated with structural modification of hesperidin. Thus, it is evident that gamma irradiation is an important technology that might modify chemical structures of various natural compounds to improve their physiological properties, such as anti-inflammation and anti-cancer activities (Byun et al., 2015, 2018).

Apoptosis, a major form of cell death, is characterized by the ability to eliminate cancer cells without damaging normal cells or tissues, under various physiological conditions (Ouyang et al., 2012; Wong, 2011). Based on this knowledge, we next investigated whether cytotoxicity induced by 150 kGy gamma-irradiated hesperidin was correlated with the apoptotic process in B16BL6 cells. The purpose was to examine whether the toxicity of 150 kGy gamma-irradiated hesperidin to B16BL6 cells was due to the induction of apoptosis. The 150 kGy hesperidin treatment resulted in higher populations of annexin V/PI-positive cells, greater weakening of cell adhesion, larger number of morphologically altered cells, and greater inhibition of cell migration than did the group treated with intact hesperidin. Furthermore, 150 kGy gamma-irradiated hesperidin induced an increase of the sub-G1 phase and depolarization of MMP through ROS generation. These

findings are consistent with other reports showing that ROS are anti-cancer agents associated with apoptotic cell death through mitochondrial pathways, and that ROS ultimately depolarizes MMP and increases the sub-G1 phase (Gackowski et al., 2002; Green, 2011; Kroemer et al., 2007).

To further define signaling pathways related to apoptotic cell death induced by 150 kGy gamma-irradiated hesperidin, we investigated apoptotic parameters, such as Bcl-2 family proteins (pro-apoptotic proteins; Bax and anti-apoptotic proteins; Bcl-2), PARP cleavage, cytochrome *c*, as well as caspase-3 and -9, as reported by previous studies conducted on the mitochondrial apoptotic pathway (Dejean et al., 2006; Hajra and Liu, 2004; Hu and Kavanagh, 2003; Wang and Youle, 2009; Waxman and Schwartz, 2003). We found that 150 kGy gamma-irradiated hesperidin induced increased Bax expression and decreased Bcl-2 expression, which subsequently triggered the release of cytochrome *c* from mitochondria into the cytosol, in addition to increasing PARP cleavage as well as the levels of caspase-3 and -9 levels in B16BL6 cells. Our findings are also consistent with other reports that ROS may induce depolarization of MMP, as well as the release of cytochrome *c* from mitochondria into the cytosol. Released cytochrome *c* triggers the activation of caspase-3 and -9, and cleaved PARP, which ultimately induces apoptosis in cancer cells (Kwon et al., 2014).

Melanoma is an aggressive cancer with metastasis that is more pronounced than any other cancer (Thang et al., 2015). Based on the foregoing results, we used mouse tumor growth and metastasis models to further clarify the anti-cancer potency of gamma-irradiated hesperidin. The 150 kGy gamma-irradiated hesperidin treatment yielded significantly greater inhibition of lung metastasis and tumor growth of melanoma B16BL6 cells in C57BL/6 mice than did the intact hesperidin; this result was similar to that of the *in vitro* mechanistic study.

The collective results we obtained suggest that structural modification of hesperidin induced by gamma irradiation may be valuable in the development of therapeutic drugs with potential for cancer treatment.

In conclusion, it is evident that gamma irradiation may play a key role in changing the structural and physiological properties of various natural compounds. The current findings indicate that the new radiolytic peak derived from 150 kGy gamma-irradiated hesperidin induced the apoptosis of murine melanoma B16BL6 cells via the ROS- and caspase-dependent mitochondrial pathway. The preventive and therapeutic effects were confirmed *in vivo* using C57BL/6 mice. Collectively, these findings may provide fundamental information vital for the development of new phytomedications using irradiation technology.

Conflicts of interest

The authors have declared no conflicts of interest.

Acknowledgments

This work was supported by the National Research Foundation of Korea grant funded by Korea government (Grant nos. 2018M2A2B3A02072069), Republic of Korea.

Transparency document

Transparency document related to this article can be found online at https://doi.org/10.1016/j.fct.2019.02.042.

References

Banjerdpongchai, R., Wudtiwai, B., Khaw-on, P., Rachakhom, W., Duangnil, N., Kongtawelert, P., 2016. Hesperidin from Citrus seed induces human hepatocellular carcinoma HepG2 cell apoptosis via both mitochondrial and death receptor pathways. Tumor Biol. 37, 227–237.

Beckett, W.S., 1993. Epidemiology and etiology of lung cancer. Clin. Chest Med. 14, 1–15.

Bi, X.L., Yang, J.Y., Dong, Y.X., Wang, J.M., Cui, Y.H., Ikeshima, T., Zhao, Y.Q., Wu, C.F., 2005. Resveratrol inhibits nitric oxide and TNF-alpha production by lipopolysaccharide-activated microglia. Int. Immunopharmacol. 5, 185–193. https://doi.org10.1016/j.intimp.2004.08.008.

Byun, E.B., Jang, B.S., Kim, H.M., Yang, M.S., Sung, N.Y., Byun, E.H., 2017. Gamma irradiation enhanced Tollip-mediated anti-inflammatory action through structural modification of quercetin in lipopolysaccharide-stimulated macrophages. Int. Immunopharmacol. 42, 157–167. https://doi.org10.1016/j.intimp.2016.11.030.

Byun, E.B., Kim, H.M., Sung, N.Y., Yang, M.S., Kim, W.S., Choi, D., Mushtaq, S., Lee, S.S., Byun, E.H., 2018. Gamma irradiation of aloe-emodin induced structural modification and apoptosis through a ROS- and caspase-dependent mitochondrial pathway in stomach tumor cells. Int. J. Radiat. Biol. 94, 403–416. https://doi.org10.1080/09553002.2018.1440330.

Byun, E.B., Sung, N.Y., Kim, J.H., Choi, J.I., Matsui, T., Byun, M.W., Lee, J.W., 2010. Enhancement of anti-tumor activity of gamma-irradiated silk fibroin via immunomodulatory effects. Chem. Biol. Interact. 186, 90–95. https://doi.org10.1016/j.cbi.2010.03.032.

Byun, E.B., Sung, N.Y., Park, J.N., Yang, M.S., Park, S.H., Byun, E.H., 2015. Gamma-irradiated resveratrol negatively regulates LPS-induced MAPK and NF-kappaB signaling through TLR4 in macrophages. Int. Immunopharmacol. 25, 249–259. https://doi.org10.1016/j.intimp.2015.02.015.

Chen, M.C., Ye, Y.Y., Ji, G., Liu, J.W., 2010. Hesperidin upregulates heme oxygenase-1 to attenuate hydrogen peroxide-induced cell damage in hepatic L02 cells. J. Agric. Food Chem. 58, 3330–3335. https://doi.org10.1021/jf904549s.

Cheung, A.F., Dupage, M.J., Dong, H.K., Chen, J., Jacks, T., 2008. Regulated expression of a tumor-associated antigen reveals multiple levels of T-cell tolerance in a mouse model of lung cancer. Cancer Res. 68, 9459–9468. https://doi.org10.1158/0008-5472.CAN-08-2634.

Choi, J.I., Kim, H.J., 2013. Preparation of low molecular weight fucoidan by gamma-irradiation and its anticancer activity. Carbohydr. Polym. 97, 358–362. https://doi.org10.1016/j.carbpol.2013.05.002.

Dejean, L.M., Martinez-Caballero, S., Manon, S., Kinnally, K.W., 2006. Regulation of the mitochondrial apoptosis-induced channel, MAC, by BCL-2 family proteins. Biochim. Biophys. Acta 1762, 191–201. https://doi.org10.1016/j.bbadis.2005.07.002.

Delmas, D., Jannin, B., Latruffe, N., 2005. Resveratrol: preventing properties against vascular alterations and ageing. Mol. Nutr. Food Res. 49, 377–395. https://doi.org10.1002/mnfr.200400098.

Filho, C.B., Del Fabbro, L., de Gomes, M.G., Goes, A.T., Souza, L.C., Boeira, S.P., Jesse, C.R., 2013. Kappa-opioid receptors mediate the antidepressant-like activity of hesperidin in the mouse forced swimming test. Eur. J. Pharmacol. 698, 286–291. https://doi.org10.1016/j.ejphar.2012.11.003.

Gackowski, D., Banaszkiewicz, Z., Rozalski, R., Jawien, A., Olinski, R., 2002. Persistent oxidative stress in colorectal carcinoma patients. Int. J. Cancer 101, 395–397. https://doi.org10.1002/ijc.10610.

Gangopadhyay, N.N., Luketich, J.D., Opest, A., Landreneau, R., Schuchert, M.J., 2014. PARP inhibitor activates the intrinsic pathway of apoptosis in primary lung cancer cells. Canc. Invest. 32, 339–348. https://doi.org10.3109/07357907.2014.919303.

Garg, A., Garg, S., Zaneveld, L., Singla, A., 2001. Chemistry and pharmacology of the citrus bioflavonoid hesperidin. Phytother Res. 15, 655–669.

Ghorbani, A., Nazari, M., Jeddi-Tehrani, M., Zand, H., 2012. The citrus flavonoid hesperidin induces p53 and inhibits NF-kappaB activation in order to trigger apoptosis in NALM-6 cells: involvement of PPARgamma-dependent mechanism. Eur. J. Nutr. 51, 39–46. https://doi.org10.1007/s00394-011-0187-2.

Gill, R.K., Vazquez, M.F., Kramer, A., Hames, M., Zhang, L., Heselmeyer-Haddad, K., Ried, T., Shilo, K., Henschke, C., Yankelevitz, D., Jen, J., 2008. The use of genetic markers to identify lung cancer in fine needle aspiration samples. Clin. Cancer Res. 14, 7481–7487. https://doi.org10.1158/1078-0432.CCR-07-5242.

Green, D.R., 2011. Means to an End: Apoptosis and Other Cell Death Mechanisms. Cold Spring Harbor Laboratory Press.

Hajra, K.M., Liu, J.R., 2004. Apoptosome dysfunction in human cancer. Apoptosis 9, 691–704. https://doi.org10.1023/B:APPT.0000045786.98031.1d.

Hu, W., Kavanagh, J.J., 2003. Anticancer therapy targeting the apoptotic pathway. Lancet Oncol. 4, 721–729.

Ilyina, A., Tikhonov, V., Albulov, A., Varlamov, V., 2000. Enzymic preparation of acid-free-water-soluble chitosan. Process Biochem. 35, 563–568.

Jung, H.J., Park, H.R., Jung, U., Jo, S.K., 2009. Radiolysis study of genistein in methanolic solution. Radiat. Phys. Chem. 78, 386–393.

Kroemer, G., Galluzzi, L., Brenner, C., 2007. Mitochondrial membrane permeabilization in cell death. Physiol. Rev. 87, 99–163.

Kwon, S.J., Lee, J.H., Moon, K.D., Jeong, I.Y., Ahn, D.U., Lee, M.K., Seo, K.I., 2014. Induction of apoptosis by isoegomaketone from Perilla frutescens L. in B16 melanoma cells is mediated through ROS generation and mitochondrial-dependent, -independent pathway. Food Chem. Toxicol. 65, 97–104. https://doi.org10.1016/j.fct.2013.12.031.

Lastra, C.A., Villegas, I., 2005. Resveratrol as an anti-inflammatory and anti-aging agent: mechanisms and clinical implications. Mol. Nutr. Food Res. 49, 405–430. https://doi.org10.1002/mnfr.200500022.

Lee, C.J., Wilson, L., Jordan, M.A., Nguyen, V., Tang, J., Smiyun, G., 2010. Hesperidin suppressed proliferations of both human breast cancer and androgen-dependent prostate cancer cells. Phytother Res. 24 (Suppl. 1), S15–S19. https://doi.org10.1002/ptr.2856.

Lee, S., Lee, M., Song, K., 2005. Effect of gamma-irradiation on the physicochemical properties of gluten films. Food Chem. 92, 621–625.

Mennen, L.I., Walker, R., Bennetau-Pelissero, C., Scalbert, A., 2005. Risks and safety of polyphenol consumption–. Am. J. Clin. Nutr. 81, 326S–329S.

Micke, O., Seegenschmiedt, M.H., German Working Group on Radiotherapy in, G., 2002. Consensus guidelines for radiation therapy of benign diseases: a multicenter approach in Germany. Int. J. Radiat. Oncol. Biol. Phys. 52, 496–513.

Natarajan, N., Thamaraiselvan, R., Lingaiah, H., Srinivasan, P., Periyasamy, B.M., 2011. Effect of flavonone hesperidin on the apoptosis of human mammary carcinoma cell line MCF-7. Biomedicine & Preventive Nutrition 1, 207–215.

Ouyang, L., Shi, Z., Zhao, S., Wang, F.T., Zhou, T.T., Liu, B., Bao, J.K., 2012. Programmed cell death pathways in cancer: a review of apoptosis, autophagy and programmed necrosis. Cell Prolif 45, 487–498. https://doi.org10.1111/j.1365-2184.2012.00845.x.

Park, H.J., Kim, M.J., Ha, E., Chung, J.H., 2008. Apoptotic effect of hesperidin through caspase3 activation in human colon cancer cells, SNU-C4. Phytomedicine 15, 147–151. https://doi.org10.1016/j.phymed.2007.07.061.

Park, J.-H., Hyun, C.-K., Shin, H.-K., Yeo, I.-H., 1997. Effects of heat treatment, sugar addition and fermentation on cytotoxicity of Korean mistletoe. Korean J. Food Sci. Technol. 29, 362–368.

Park, J.-N., Byun, E.-B., Kim, J.-J., Jang, B.-S., Park, S.-H., 2015. Induction of apoptosis by gamma-irradiated apigenin in H1975 human non-small lung cells. J.J.Korean Soc. Food Sci. Nutr. 44, 816–822.

Seegenschmiedt, M.H., Katalinic, A., Makoski, H., Haase, W., Gademann, G., Hassenstein, E., 2000. Radiation therapy for benign diseases: patterns of care study in Germany. Int. J. Radiat. Oncol. Biol. Phys. 47, 195–202.

So, F.V., Guthrie, N., Chambers, A.F., Moussa, M., Carroll, K.K., 1996. Inhibition of human breast cancer cell proliferation and delay of mammary tumorigenesis by flavonoids and citrus juices. Nutr. Canc. 26, 167–181. https://doi.org10.1080/01635589609514473.

Sung, N.-Y., Byun, E.-B., Song, D.-S., Jin, Y.-B., Kim, J.-K., Park, J.-H., Song, B.-S., Jung, P.-M., Byun, M.-W., Lee, J.-W., 2013. Effect of gamma irradiation on mistletoe (Viscum album) lectin-mediated toxicity and immunomodulatory activity. FEBS open bio 3, 106–111.

Sung, N.-Y., Byun, E.-B., Song, D.-S., Jin, Y.-B., Park, J.-N., Kim, J.-K., Park, J.-H., Song, B.-S., Park, S.-H., Lee, J.-W., 2014. Anti-inflammatory action of γ-irradiated genistein in murine peritoneal macrophage. Radiat. Phys. Chem. 105, 17–21.

Sung, N.-Y., Byun, E.-H., Kwon, S.-K., Song, B.-S., Choi, J.-i., Kim, J.-H., Byun, M.-W., Yoo, Y.-C., Kim, M.-R., Lee, J.-W., 2009. Immune-enhancing activities of low molecular weight β-glucan depolymerized by gamma irradiation. Radiat. Phys. Chem. 78, 433–436.

Thang, N.D., Yajima, I., Kumasaka, M.Y., Iida, M., Suzuki, T., Kato, M., 2015. Deltex-3-like (DTX3L) stimulates metastasis of melanoma through FAK/PI3K/AKT but not MEK/ERK pathway. Oncotarget 6, 14290–14299. https://doi.org10.18632/oncotarget.3742.

Wang, C., Youle, R.J., 2009. The role of mitochondria in apoptosis. Annu. Rev. Genet. 43, 95–118.

Waxman, D.J., Schwartz, P.S., 2003. Harnessing apoptosis for improved anticancer gene therapy. Cancer Res. 63, 8563–8572.

Wong, R.S., 2011. Apoptosis in cancer: from pathogenesis to treatment. J. Exp. Clin. Cancer Res. 30, 87.

Wu, C.C., Bratton, S.B., 2013. Regulation of the intrinsic apoptosis pathway by reactive oxygen species. Antioxidants Redox Signal. 19, 546–558. https://doi.org10.1089/ars.2012.4905.

Wu, Y., Zhao, D., Zhuang, J., Zhang, F., Xu, C., 2016. Caspase-8 and caspase-9 functioned differently at different stages of the cyclic stretch-induced apoptosis in human periodontal ligament cells. PLoS One 11, e0168268. https://doi.org10.1371/journal.pone.0168268.